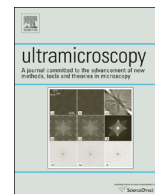




ELSEVIER

Contents lists available at ScienceDirect

Ultramicroscopy

journal homepage: www.elsevier.com/locate/ultramic

A numerical model for multiple detector energy dispersive X-ray spectroscopy in the transmission electron microscope

W. Xu, J.H. Dycus, X. Sang, J.M. LeBeau*

Department of Materials Science and Engineering, North Carolina State University, Raleigh, NC 27695, USA

ARTICLE INFO

Article history:

Received 23 June 2015

Received in revised form

13 February 2016

Accepted 18 February 2016

Keywords:

Energy dispersive X-ray spectroscopy (EDS)

Super-X

Detector collection angle

X-ray absorption correction

Shadowing

Spurious X-rays

ABSTRACT

Here we report a numerical approach to model a four quadrant energy dispersive X-ray spectrometer in the transmission electron microscope. The model includes detector geometries, specimen position and absorption, shadowing by the holder, and filtering by the Be carrier. We show that this comprehensive model accurately predicts absolute counts and intensity ratios as a function of specimen tilt and position. We directly compare the model to experimental results acquired with a FEI Super-X EDS four quadrant detector. The contribution from each detector to the sum is investigated. The program and source code can be downloaded from <https://github.com/subangstrom/superAngle>.

© 2016 Elsevier B.V. All rights reserved.

1. Introduction

Energy Dispersive X-ray Spectroscopy (EDS) is widely used for qualitative and quantitative elemental composition analysis at the nanometer scale [1]. Recent developments have focused on improving the X-ray signal collection efficiency by either adding more detectors or using a larger collection area [2]. For example, the FEI Super-X system incorporates four windowless 30 mm² SDD detectors that are placed symmetrically around the optic axis. The total collection angle of such systems is 0.7 or 0.9 sr depending on the pole piece geometry [3,4]. Furthermore, the use of windowless detectors in this configuration further increases the collection efficiency for light elements [5,6].

Advances in EDS detector technology, paired with high brightness of field emission guns and aberration-correction, have enabled routine atomic-resolution EDS elemental mapping. With this capability, attention has turned to quantifying elemental composition on an atom column by atom column basis [7–13]. Beyond accounting for the complexities of electron channeling, quantitative atomic resolution elemental mapping also requires knowledge of detector collection solid-angle [13]. When the sample is tilted however, e.g. to zone axis condition necessary for atomic resolution, the full collection solid angle can be reduced if the specimen holder shadows the detector [14,15].

In the Super-X configuration, at least one of the four detectors will be inevitably blocked or shadowed as the sample holder tilt increases. Furthermore, specimen shift can play a role in determining which X-rays are collected. Beyond the holder and sample, the Be specimen carrier can also absorb a significant fraction of the X-ray signal, especially for light elements. Rather than an absolute number, the effective collection solid angle will change as the sample is tilted and/or shifted, which cannot be accounted for from calibration alone. As a result, absolute EDS quantification at the atomic scale becomes even more challenging. Instead, a sufficiently complex theoretical model to predict the variation of effective collection angle or absorption correction factors with the specimen tilt and shift would provide critical insights and information. Recently, Yang et al. [16] have provided analytical solutions for absorption correction in the Super-X configuration while Yeoh et al. considered the effects of holder shadowing in EDS tomography [15]. Slater et al. also reported optical measurements of a tomography holder to better integrate holder geometry in EDS tomography quantification [17]. A more complete model, however, is still lacking.

In this work, a comprehensive numerical model that includes the precise geometry of the specimen holder to determine the combined effects of specimen absorption, Be holder absorption, and holder shadowing is developed. We find that when tilting the specimen, the geometric variance between the specimen and each detector introduces important contributions that should be taken into account, particularly when tilting beyond even 10°.

* Corresponding author.

E-mail address: jmlebeau@ncsu.edu (J.M. LeBeau).

Furthermore, using Ni₃Al as a test case, we validate the model by directly comparing total absolute counts and intensity ratios from experiment with those calculated with the model. Through the model, we provide fundamental insights into the complexities of how X-rays reach each detector as a function of tilt and position. The results provide important input to achieve accurate quantification as detector geometries become increasingly complex.

2. Materials & methods

Samples of Ni₃Al were prepared either by wedge polishing or focused ion beam (FIB). The wedge polished sample was first mechanically thinned with an Allied Multiprep system using diamond lapping films, and subsequently ion-milled to electron transparency with a Fischione 1050 ion mill. The FIB sample was prepared using an FEI Quanta 3D FEG dual-beam instrument, which was directly cut from a bulk sample and attached in the middle of 'M' shaped PELCO® Mo grid. The sample was then further thinned using 30 kV Ga⁺ ions that was then stepped down to 5 kV and 2 kV for final polishing.

A probe-corrected FEI Titan G2 microscope operated at 200 kV and equipped with a four-quadrant FEI Super-X detector was used throughout. A FEI low background double tilt specimen holder (LB DT HiVis specimen holder FP6595/20) was used. EDS spectra were acquired along X- and Y-tilt axes using an area of about 200 × 200 nm² to reduce beam damage and carbon contamination. At each specimen tilt, the signal on each of the four Super-X detector segments was acquired individually. The probe current, measured using a calibrated CCD, was approximately 121 and 95 pA for the wedge-polished and FIB samples respectively. The CCD was calibrated using a picoammeter, with a precision of about 0.1 pA, connected to the EELS drift tube. The EDS acquisition rate was in the range of 0.1–1.7 kcps per detector depending on the tilt. For each spectrum, the live time was 69 and 135 s for FIB and wedge-polished samples respectively. Note that, the live time τ was different from the total experimental acquisition time, influenced by the dwell time for each pixel. Strong electron channeling conditions were avoided. Furthermore, the acquisition area was kept approximately constant. For the wedge-polished specimen, the acquisition position was at approximately –0.11 mm, –0.12 mm and 0.29 mm along x, y and z directions relative to the optic axis, respectively. The FIB sample was shifted 0.37 mm, 0.02 mm and 0.22 mm along x, y and z, respectively.

The tilt series data were acquired at approximately the same thickness, as monitored by electron energy loss spectroscopy (EELS) with a collection semi-angle of 39 mrad. Compared to using a constant location, this strategy largely reduced the possible position variation or uncertainty during the X/Y tilt experiment. The sample thickness was kept at a constant value of 1.0 inelastic mean free path for the wedge-polished sample, and 1.5 inelastic mean free paths for the FIB sample. This corresponds to thicknesses of 84 and 126 nm for the wedge-polished and FIB samples, respectively, as estimated from the Malis model with error of approximately ± 10% [18,19].

3. Description of the numerical model

Fig. 1a shows a geometric overview of a FEI Super-X detector, with the specimen placed at the origin. Four detectors are symmetrically placed about the sample with a polar angle, $\theta = 18^\circ$, and azimuth angles, φ_D , of 135°, 45°, 315°, 225°. To discretize the detector, differential elements are given by $d\theta$ and $d\varphi$, as in Fig. 1b. A factor of $\sin \theta_i$ is included to normalize the intensity of each X-ray. Note that the index i indicates a discrete X-ray detector element,

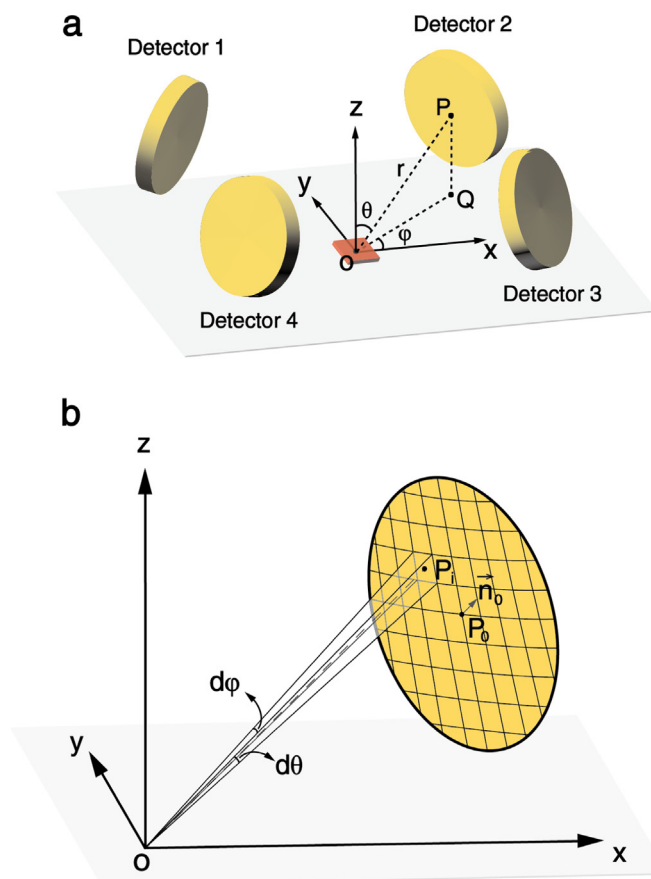


Fig. 1. (a) Super-X detector quadrants placed symmetrically about the sample. The specimen is placed at the origin point, O, at distance r from the detectors. P and Q define points within each detector plane and projected onto the specimen plane, respectively. (b) X-rays generated within the specimen are discretized onto the detector surface, defined by surface normal \mathbf{n}_0 , within differential solid angle elements centered about points P_i .

or equivalently a X-ray trajectory from the sample. The solid angle for each differential detector element is then:

$$d\Omega = d\theta d\varphi \sin \theta_i \quad (1)$$

After discretization, only those X-rays that pass into the detector area are considered. Based on the central point, P_i , that each X-ray passes through a detector, we define the plane normal of that detector in spherical coordinates to be $\mathbf{n} = [1, \theta_D + \delta_D, \varphi_D]$ where δ_D is the angle that the detector could be tilted along the $\mathbf{OP} \times \mathbf{PQ}$ direction,

$$(\mathbf{OP}_i - \mathbf{OP}_0) \cdot \mathbf{n} = 0 \quad (2)$$

By solving Eq. (2), we obtain a large set of intercept coordinates (P_i) from the X-rays that pass through the detector plane. This process is then repeated for each of the four different detectors. By considering only those intercepts with $|\mathbf{P}_i \mathbf{P}_0|$ less than the detector radius, the complete set of the X-rays, \mathbf{OP}_i , that can be collected by the detectors is determined. For convergence, $d\theta$ and $d\varphi$ intervals of 0.2° are sufficient to fully describe the detectors. Note that this numerical approach can be used to accommodate any arbitrary number of detectors or detector shape by modifying the above criteria.

As the nominal total solid angle is 0.7 sr for the Super-X system, the distance from the specimen to the center of the detector $|\mathbf{OP}_0|$ is approximately 12.0 mm. Here, we consider only the collimated area of the detector (26.4 mm²), i.e. active detector radius of 2.9 mm [20], and a detector elevation angle of 18° (or $\theta_D = 72^\circ$). δ_D

Download English Version:

<https://daneshyari.com/en/article/8037915>

Download Persian Version:

<https://daneshyari.com/article/8037915>

[Daneshyari.com](https://daneshyari.com)